Supporting Information

Strain Engineering in Single-Atom Catalysts: $GaPS_4$ for Bifunctional Oxygen Reduction and Evolution

Xuefei Liu[1], *Tianyun Liu*[1], *Wenjun Xiao*[1], *Wentao Wang*[2*], *Yuefei Zhang*[1], *Gang Wang*[1], *Zijiang Luo*[3]*, *Jin-Cheng Liu*[4]*

[1] School of Physics and Electronic Science, Guizhou Normal University, Guiyang 550025, China.

[2] Guizhou Provincial Key Laboratory of computational Nano-Material Science, Guizhou Education University, Guiyang 550018, China.

[3] College of Information, Guizhou University of Finance and Economics, Guiyang 550025, China.

[4] Department of Chemistry and Key Laboratory of Organic Optoelectronics & Molecular Engineering of Ministry of Education, Tsinghua University, Beijing 100084, China

*Corresponding Authors. Email: wuli8@163.com (W. W.); luozijiang@mail.gufe.edu.cn (Z. L.); liujinchengcheng@hotmail.com (J.-C. L.)

Table of contents

Note S1 The details of OER/ORR process

For the OER process, in the first step, transition metal@V_{S1}-$GaPS_4$ (denoted as *) takes one H_2O molecule from the solvent and releases one ($H^+ + e^-$) pair, leading to the formation of *OH. In the second step, *OH continues to dissociate to *O and one ($H^+ + e^-$) pair. Then the third step, another H_2O molecule reacts with the *O to form *OOH with the release of one ($H^+ + e^-$) pair. The last step is the final product of O_2 and the O_2 molecule will release from the surface of the catalyst with one ($H^+ + e^-$) pair released. The four elementary steps of OER can be described as:

$$H_2O + * \rightarrow *OH + (H^+ + e^-) \tag{S1}$$

$$*OH \rightarrow *O + (H^+ + e^-) \tag{S2}$$

$$H_2O + *O \rightarrow *OOH + (H^+ + e^-) \tag{S3}$$

$$*OOH \rightarrow * + O_2 + (H^+ + e^-) \tag{S4}$$

where $*$, H^+, e^- denotes transition metal@V_{S1}-$GaPS_4$ substrate, proton, and electron, respectively, and $*OH$, $*O$, $*OOH$ represent three different catalytic intermediates.

The ORR process can be treated as the inverse process of the OER:

$$O_2 + * + (H^+ + e^-) \rightarrow *OOH \tag{S5}$$

$$*OOH + (H^+ + e^-) \rightarrow H_2O + *O \tag{S6}$$

$$*O + (H^+ + e^-) \rightarrow *OH \tag{S7}$$

$$*OH + \left(H^+ + e^-\right) \rightarrow H_2O + * \tag{S8}$$

To avoid calculating the free energy of O_2 gas, the experimental reaction energy of $2H_2O \rightarrow O_2 + 2H_2$ (4.92 eV) was considered. Moreover, By reference of the standard hydrogen electrode potential, we can relate the chemical potential ($H^+ + e^-$) pair to that of $1/2H_2$ under standard condition[1]. Accordingly, the free energy change of each step can be expressed as:

$$\Delta G_1 = \Delta G_{*OH} - eU + \Delta G_{H+}(pH) \quad (S9)$$

$$\Delta G_2 = \Delta G_{*O} - \Delta G_{*OH} - eU + \Delta G_{H+}(pH) \quad (S10)$$

$$\Delta G_3 = \Delta G_{*OOH} - \Delta G_{*O} - eU + \Delta G_{H+}(pH) \quad (S11)$$

$$\Delta G_4 = 4.92 - \Delta G_{*OOH} - eU + \Delta G_{H+}(pH) \quad (S12)$$

Where ΔG_{*OH}, ΔG_{*O}, and ΔG_{*OOH} represent the free energy change of *OH, *O, and *OOH intermediate, respectively. ΔG is the Gibbs free energy difference of each elemental step, defined as:

$$\Delta G = \Delta E_{*DFT} + \Delta E_{ZPE} + T\Delta S \quad (S13)$$

E_{*DFT}, E_{ZPE}, T, and ΔS represent the energy calculated from DFT calculation, zero-point energy correction, temperature, and entropy correction. The ZPE and $T\Delta S$ of adsorbed species are listed in **Table S1**. U is the potential measured against normal hydrogen electrode (NHE) at standard conditions (T = 298.15 K, P = 1 bar, pH = 0). The free energy change of the protons relative to the NHE at non-zero pH is described by the Nernst equation as $\Delta G_{H+}(pH) =-k_B T\ln(10) \times pH$.

The energy differences of the corresponding intermediates are expressed as:

$$\Delta E_{DFT}(*OH) = E_{DFT}(*OH) - E_{DFT}(*) - [E_{DFT}(H_2O) - \frac{1}{2}E_{DFT}(H_2)] \quad (S14)$$

$$\Delta E_{DFT}(*O) = E_{DFT}(*O) - E_{DFT}(*O) - [E_{DFT}(H_2O) - E_{DFT}(H_2)] \quad (S15)$$

$$\Delta E_{DFT}(*OOH) = E_{DFT}(*OOH) - E_{DFT}(*) - [2E_{DFT}(H_2O) - \frac{3}{2}E_{DFT}(H_2)] \quad (S16)$$

Where the E_{DFT} (*OH), E_{DFT} (*O), E (*), E_{DFT} (H_2O), and E_{DFT} (H_2) indicate the total energy of *OH, *O, substrate, H_2O molecular, H_2 molecular, separately.

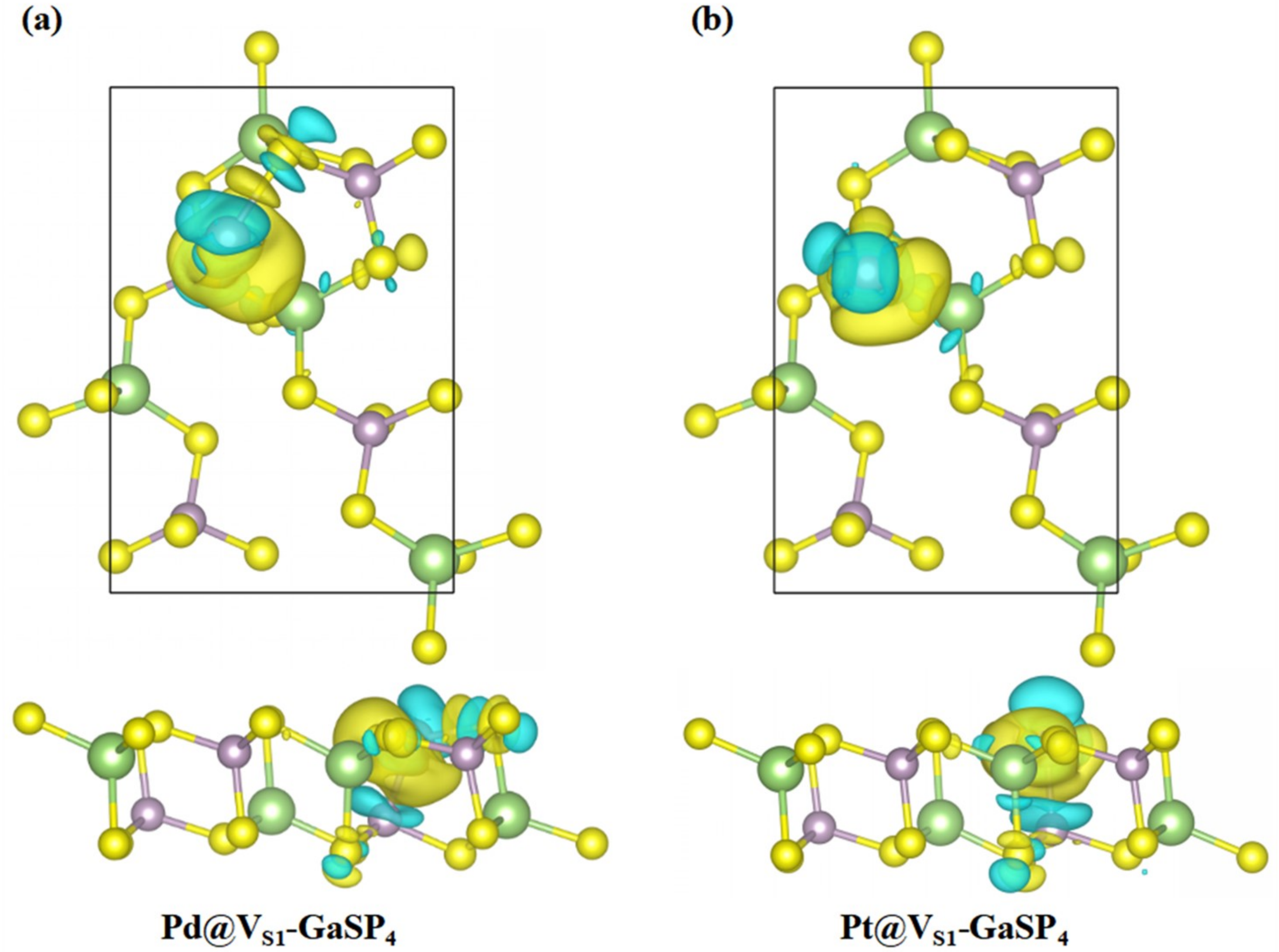

Figure S1: Top and side view of charge density difference between Pd in Pd@V$_{S1}$-GaPS$_4$ (a) as well as Pt in Pt@V$_{S1}$-GaPS$_4$(b) and V$_{S1}$-GaPS$_4$ substrate. Mauve and yellow regions are the charge accumulation region and depletion region. The isosurface value is set to 0.0025 e/Å^3.

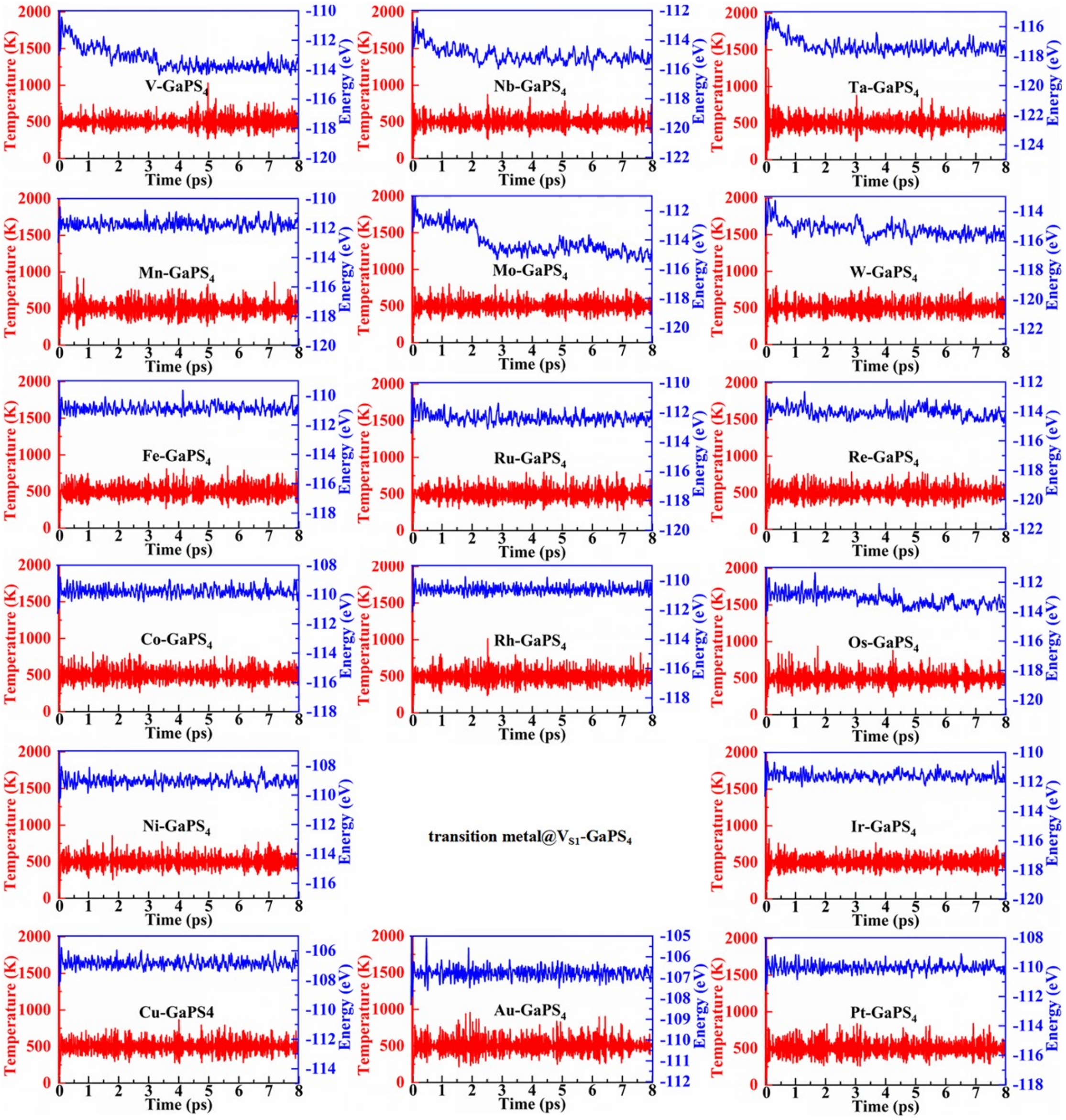

Figure S2. Evolution of the total energy and temperature for transition metal@V_{S1}-$GaPS_4$ (transition metal=Au, Co, Cu, Fe, Ir, Mn, Mo, Nb, Ni, Os, Pt, Re, Rh, Ru, Ta, V, W), the time lasts for 8 ps at 500 K.

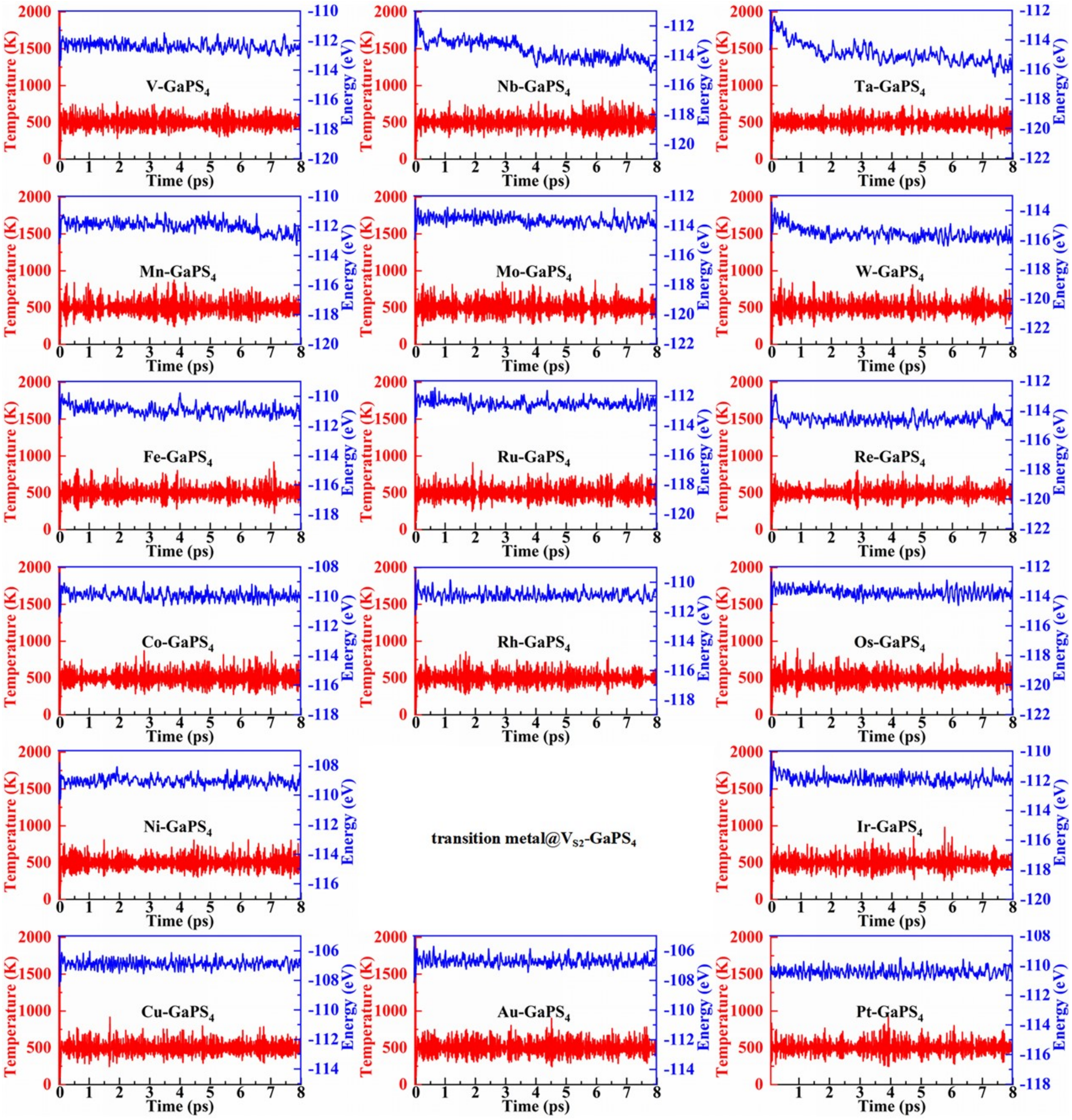

Figure S3. Evolution of the total energy and temperature for transition metal@V_{S2}-$GaPS_4$ (transition metal=Ag, Au, Co, Cr, Cu, Fe, Ir, Mn, Mo, Nb, Ni, Os, Pd, Pt, Re, Rh, Ru, Ta, Tc, V, W), the time lasts for 8 ps at 500 K.

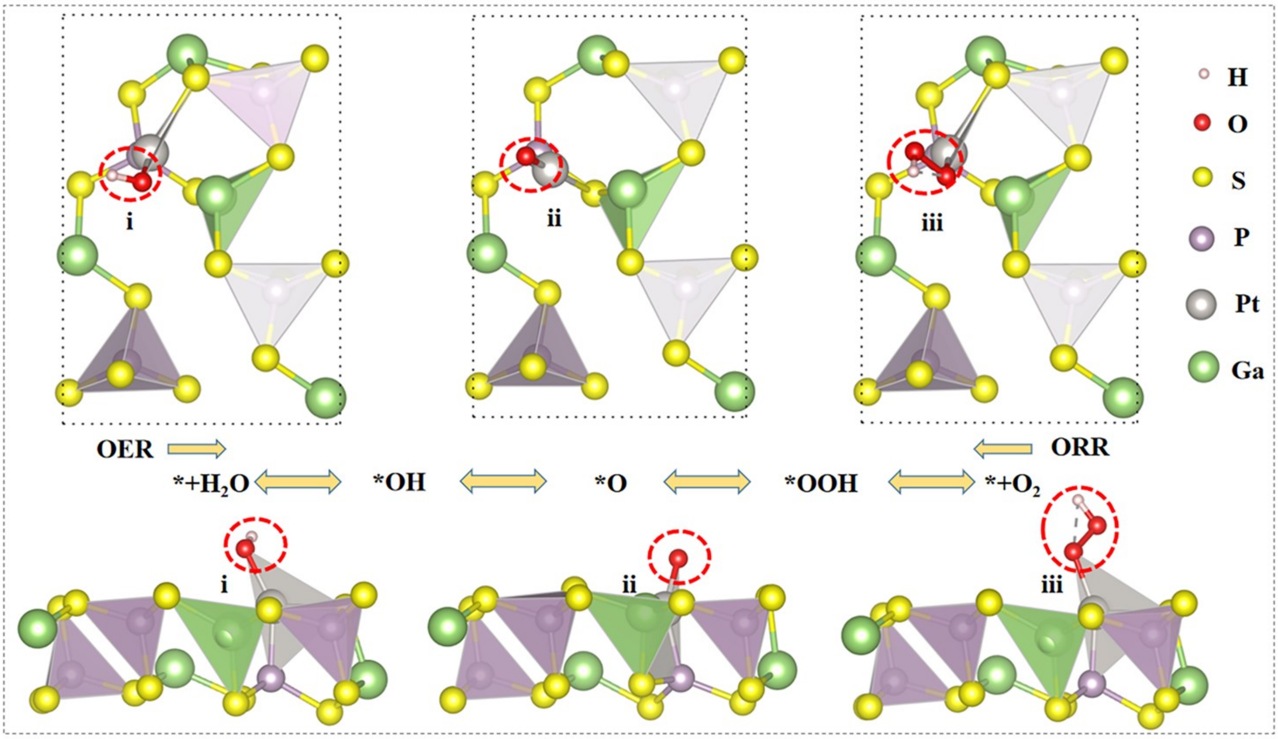

Figure S4. Geometry of the intermediate of OER (from left to right) and ORR (from right to left) of Pt@V$_{S1}$-GaPS$_4$ system.

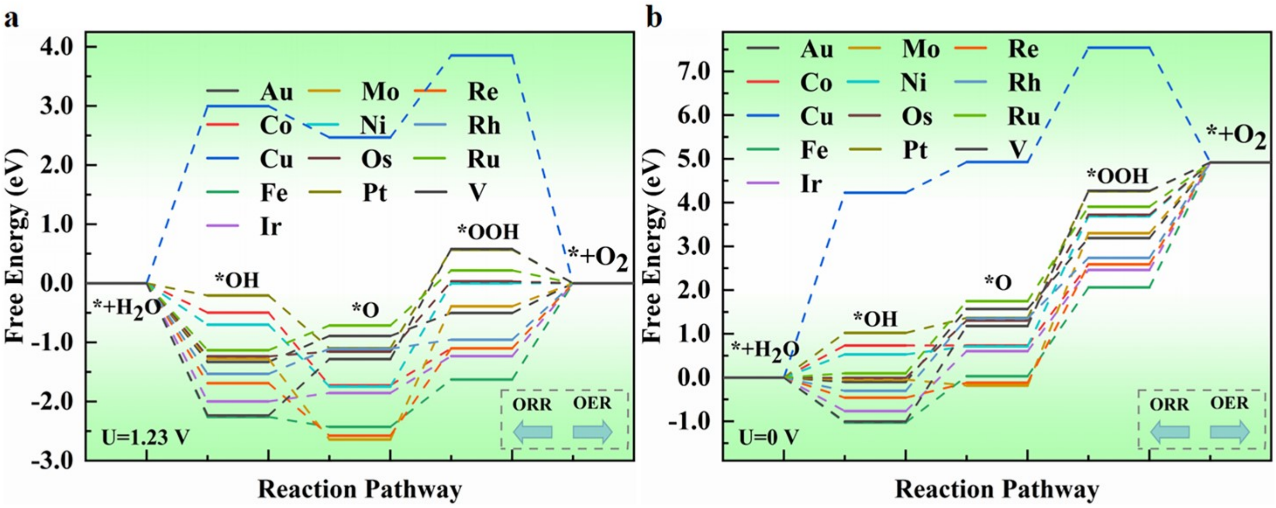

Figure S5: OER and ORR free energy steps of the transition metal@V$_{S2}$-GaPS$_4$ (transition metal=Ag, Au, Co, Cr, Cu, Fe, Ir, Mn, Mo, Nb, Ni) system under the potential U = 1.23 V (a), U= 0 V(b), respectively. The OER reaction process is from the left to the right while the ORR is contrary to the OER progress.

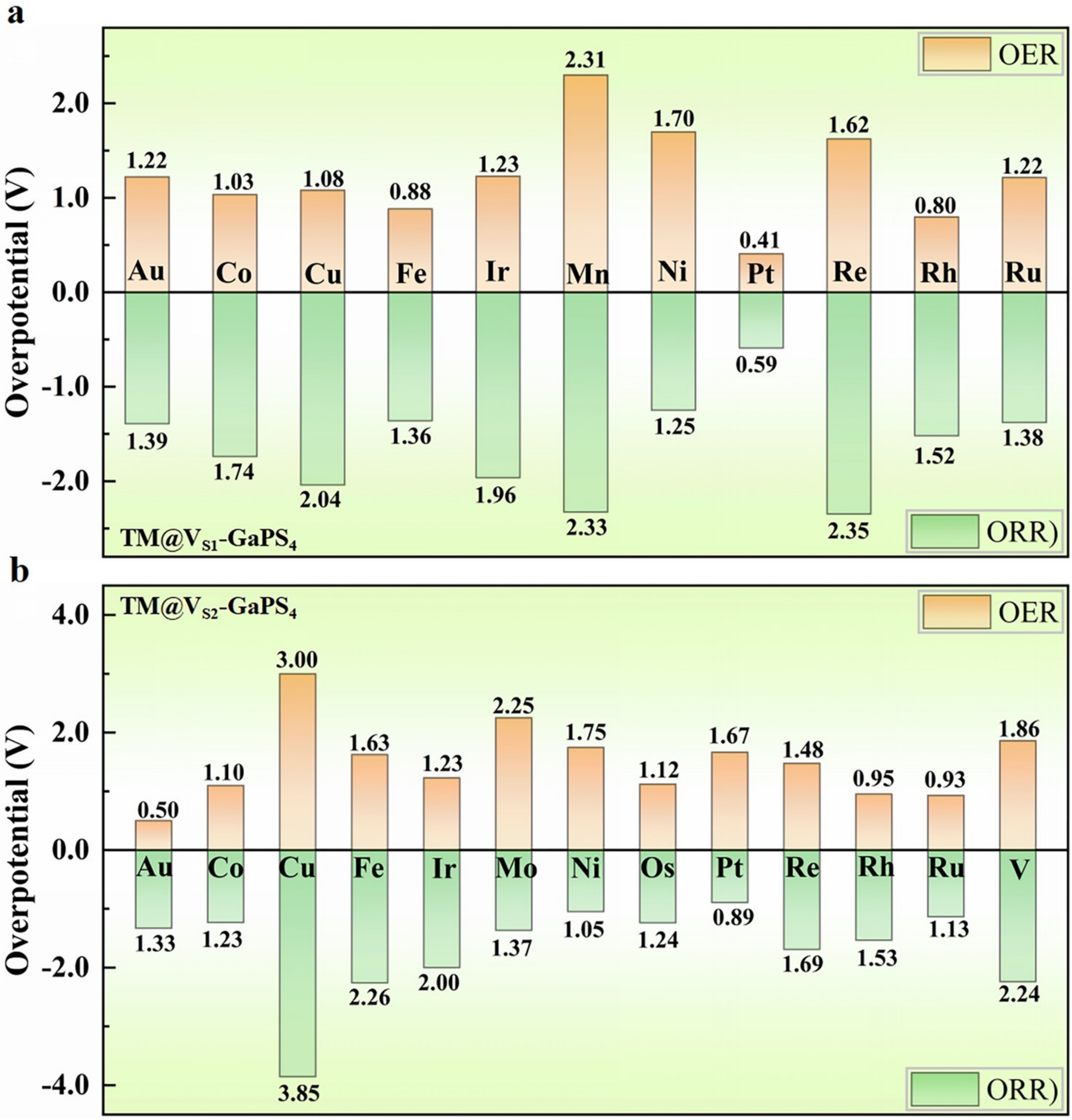

Figure S6. Histogram of OER/ORR overpotential (in V) of transition metal@V$_{S1}$-GaPS$_4$ systems (transition metal = Au, Co, Cu, Fe, Ir, Mn, Ni, Pt, Re, Rh, Ru) (a), transition metal@V$_{S2}$-GaPS$_4$ system (from Ag to W) (b).

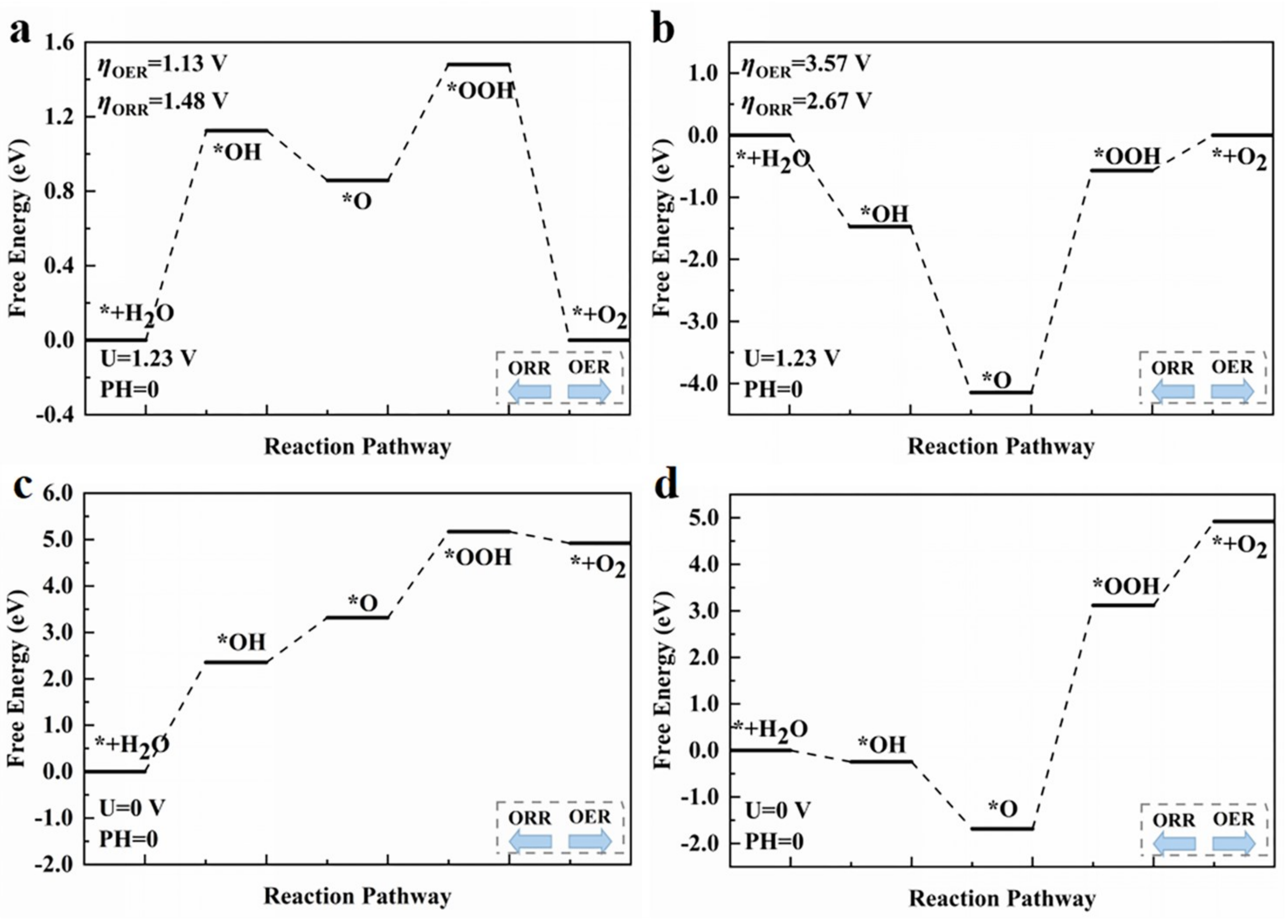

Figure S7. Free energy change of OER and ORR of the pure two-dimensional $GaPS_4$ under PH = 0, U=1.23 V (a), PH = 0,U = 0 V(c). Free energy change of OER and ORR process for transition metal@V_{S1}-$GaPS_4$ under PH = 0, U=1.23 (b), PH=0,U = 0 V (d).

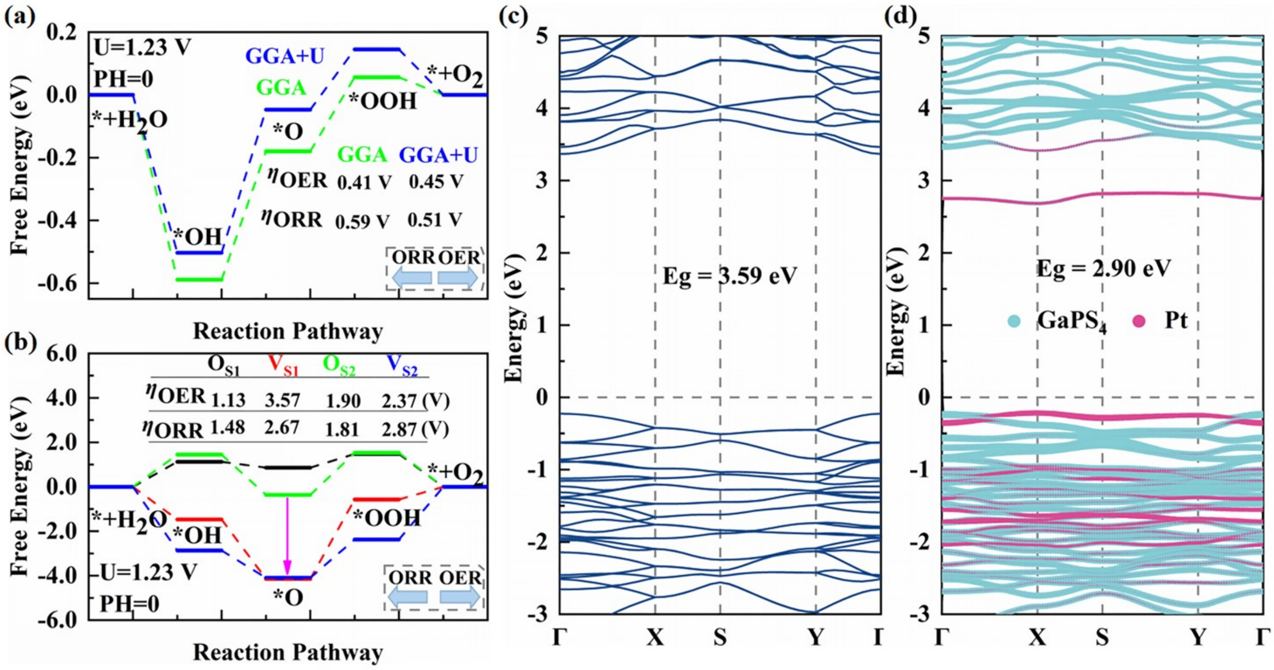

Figure S8. Free Energy changes of for Pt@V_{S1}-$GaPS_4$ under GGA calculation and GGA+U calculation (a). The overpotentials of OER/ORR for Pt-based systems are corrected to be 0.45/0.51 V. The corresponding overpotentials under the pure GGA method are 0.41/0.59 V. The negligible change of OER and ORR overpotential values indicates that our results for other substrates without GGA+U are reliable. The free energy change for pure and vacant $GaPS_4$ system without transition metal (b). The Heyd−Scuseria−Ernzerhof hybrid functional band structure of $GaPS_4$ (c) and Pt doped $GaPS_4$ (d).

Note S2 The clustering possibility

Strong interactions between transition metal atoms and the substrate are required to prevent single atoms from aggregating into nanoparticles[2]. Therefore, to study the clustering possibility of transition metal atom on $GaPS_4$, we consider the cluster energy ($E_{cluster} = E_{bind} - E_{coh}$) is taken into consideration, where E_{coh} represents the cohesive energy of transition metal atoms. The cohesive energy of bulk transition metal is defined as[3]:

$$E_{coh} = E_{transition\ metal\ \text{- bulk}}/n - E_{transition\ metal\ \text{- single}} \tag{S17}$$

$E_{transition\ metal\ \text{- bulk}}$ represent the total energy of isolated transition metal atom in a vacuum and transition metal bulk, the number of transition metal atoms in bulk is represented by n. Furthermore, the dissolution possibility of the transition metal@V_{S1}(V_{S2})-$GaPS_4$ system can be studied by calculating the dissolution potential[4, 5]. Here, the dissolution potential is defined as[6]:

$$U_{diss} = U_{diss\ \text{- bulk}} - E_{cluster}/n_e \tag{S18}$$

The U_{diss} and $U_{diss\text{-}bulk}$ are the dissolution potential of transition metal@V_{S1}-$GaPS_4$ system and transition metal bulk phase, respectively. The n_e represents the number of electrons transferred during dissolution. Theoretically, the negative cluster energy and positive dissolution potential of the transition metal@V_{S1}-$GaPS_4$ system indicates that the system has good thermodynamic and electrochemical stability. As depicted in **Figure S9** and **Table S4**, the Pt@V_{S1}(V_{S2})-$GaPS_4$ systems can exist thermodynamically and electrochemically, while other transition metal-doped systems may form transition metal clusters.

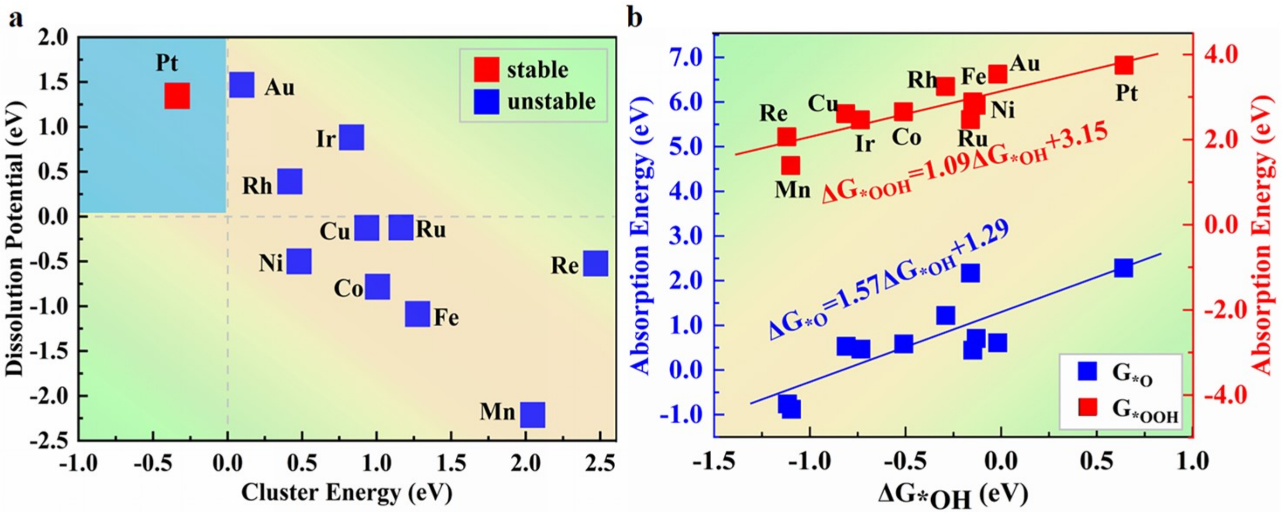

Figure S9.Transition metals' cluster energy and dissolution potential in transition metal@V_{S1}-$GaPS_4$ (a). The criteria of cluster < 0 and dissolution potential > 0 indicate the thermodynamical and electrochemical stability of the transition metal@$GaPS_4$ system. the scaling relation between ΔG_{*OOH}(ΔG_{*O}) and ΔG_{*OH} of the different transition metal based systems (b).

Note S3 The projected crystal orbital Hamilton population

The interactions of the transition metal-d orbital and the electronic states of adsorbates will be accompanied by the formation of the bonding and antibonding states (**Figure S10 a**). This means that the d-orbital of the transition metal atom interacts with the S-2p orbital electrons and divides the energy levels into two parts, both the bonding states below the Fermi level and the antibonding states above the Fermi level are occupied. Thus, the projected crystal orbital Hamilton population (pCOHP) calculation is introduced to analyze the bonding and antibonding states after the OH intermediate is absorbed on transition metal@V_{S1}-$GaPS_4$, as seen in **Figure S11**. The bonding and antibonding states are distributed on the right and left sides. Taking the Pt@V_{S1}-$GaPS_4$ as an example, it is worth noting that the adsorption strength will be weakened as many antibonding orbitals are below E_F. In addition, a large splitting means a strong interaction between d-band electrons from Pt and S-p electrons. Consequently, Pt@V_{S1}-$GaPS_4$ shows to be an ideal electrocatalyst for the OER/ORR process.

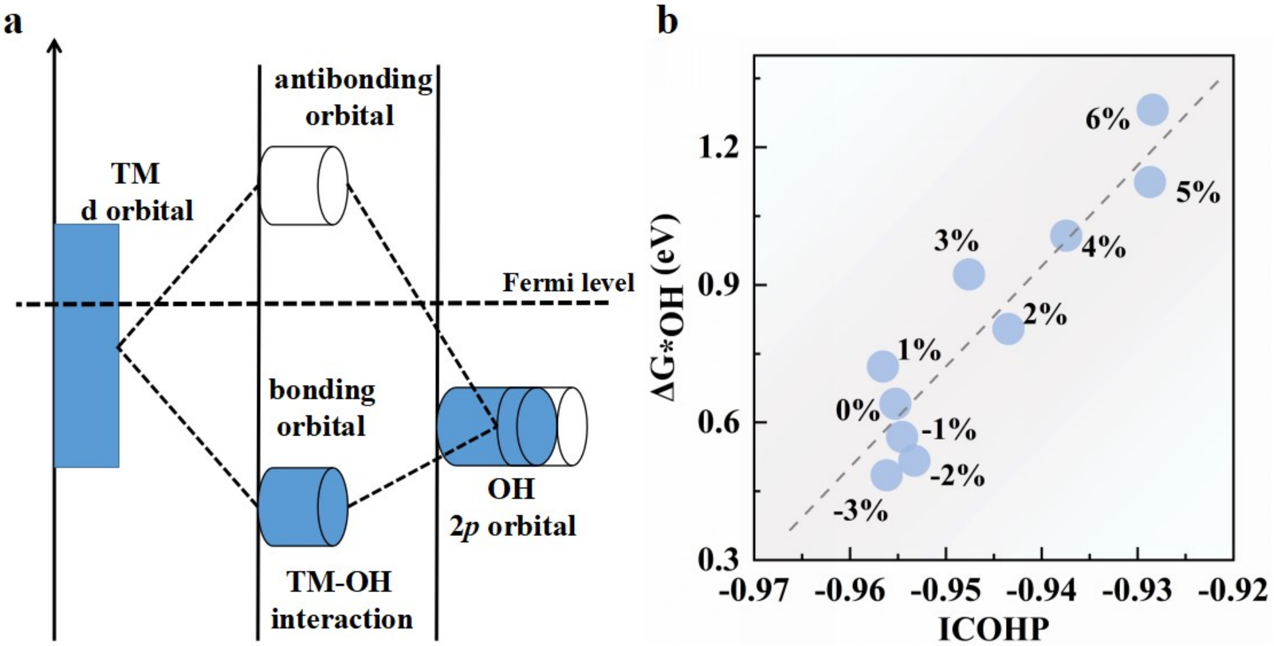

Figure S10. Schematic diagram of the interaction between d orbital electrons of transition metal and

P orbital electrons of adsorption molecule OH on transition metal@$V_{S1/S2}$-$GaPS_4$ (a). The linear relationship between the value of the ICOHP under different strains of Pt@V_{S1}-$GaPS_4$ and the adsorption energy of OH (b).

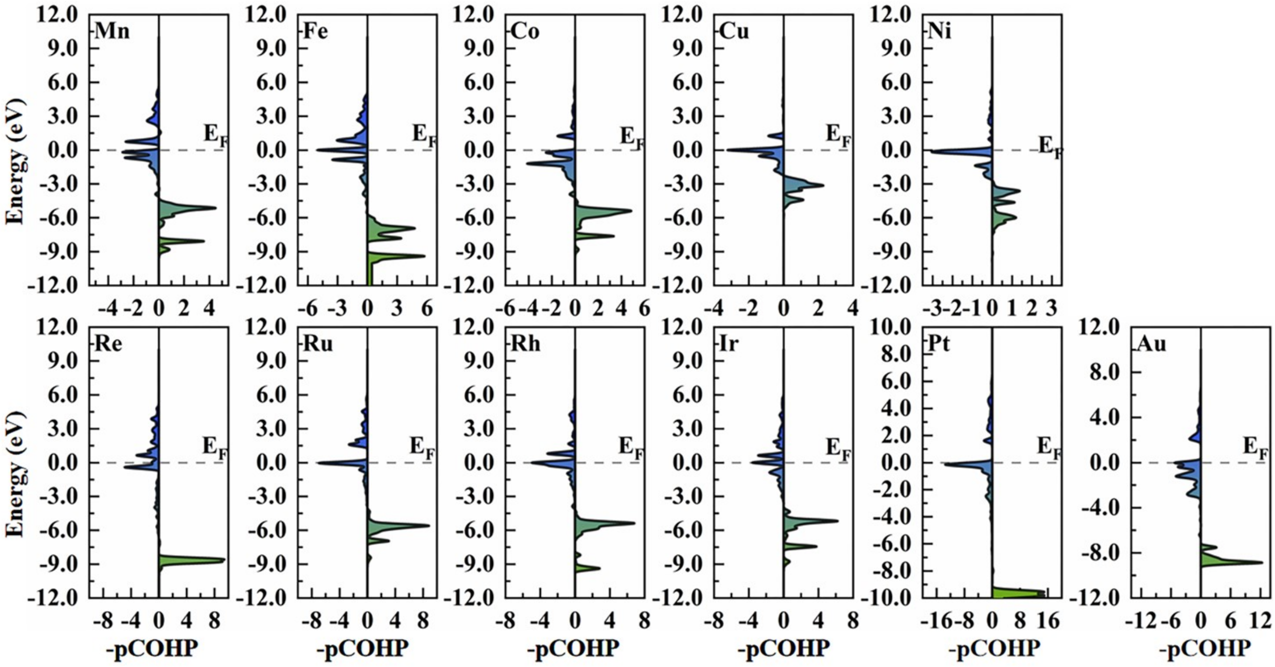

Figure S11. Projected crystal orbital Hamilton population (pCOHP) between transiton metal center and OH intermediate. E_F denotes the Fermi level. The bonding and antibonding contributions are displayed on the right and left, respectively.

Note S4 Machine learning

Machine learning (ML) is based on the gradient boosted regression (GBR) algorithm[7, 8]. The training set D = {(x_1, y_1), (x_2, y_2), … (x_n, y_n)} is divided into J disjoint parts, where J is the number of leaf nodes in every regression tree. To minimize the loss function L, the decision tree parameter θ_m is defined as:

$$\theta_m = \mathrm{argmin}_\theta \sum_{i=1}^{n} L(y_i, f_{m-1}(x_i) + t_m(x_i)) \tag{S19}$$

where $t_m(x)$, $f_{m\text{-}1}(x)$ is the m_{th} and the $(m\text{-}1)_{th}$ regression tree function after iterations.

The GBR training process is summarized by four steps: (i) initializing a regression tree function

$\mathrm{argmin}_c\sum_{i=1}^{n}L(y_i,c)$ Where c is a constant number. (ii) Calculate the negative gradient of the loss function as the estimated residual value $r_{mi} =- \left[\partial L(y_i,f(x_i)/\partial f(x_i)\right]_{f(x) = f_{m-1}(x)}$. (iii) Use the new data set (x_i, r_{mi}) to obtain the updated regression tree function $f_m(x)$. (iv) Repeat steps (ii) and (iii) to reach the final regression model, which is determined by:

$$f_M(x) = \sum_{m=1}^{M} t(x;\theta_m) \tag{S20}$$

The prediction accuracy of GBR is described by the coefficient of determination (R^2) and root-mean-square error(RMSE), defined as:

$$R^2 = 1 - \frac{\frac{1}{n}\sum_{i=1}^{n}(y_i - \hat{y}_i)^2}{\frac{1}{n}\sum_{i=1}^{n}(y_i - \mu_i)^2} \tag{S21}$$

$$RMSE = \sqrt{\frac{1}{n}\sum_{i=1}^{n}(y_i - \hat{y}_i)^2} \tag{S22}$$

in which y_i and $\hat{y}_i$ are the sample label value and the predicted value based on GBR model, respectively. Usually, a higher R^2 and a lower RMSE means a more precise GBR model.

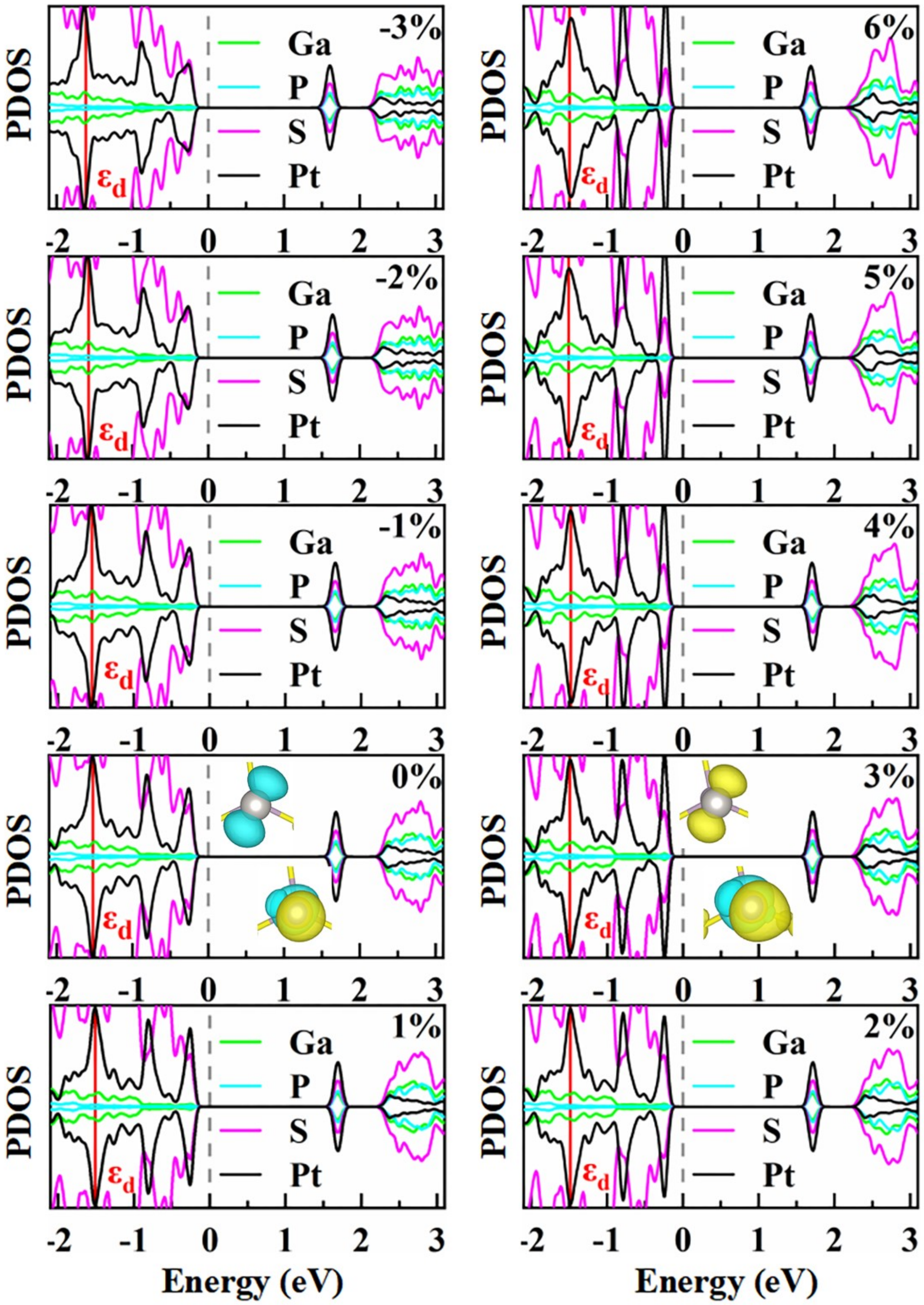

Figure S12. Partial density of Pt@V$_{S1}$-GaPS$_4$ system, the Fermi level is set to zero, ε_d is the d-orbital center of Pt by applied biaxial strain. The insert in 0% and 3% is the occupied or unoccupied d-orbital wavefunction of Pt most near the Fermi level.

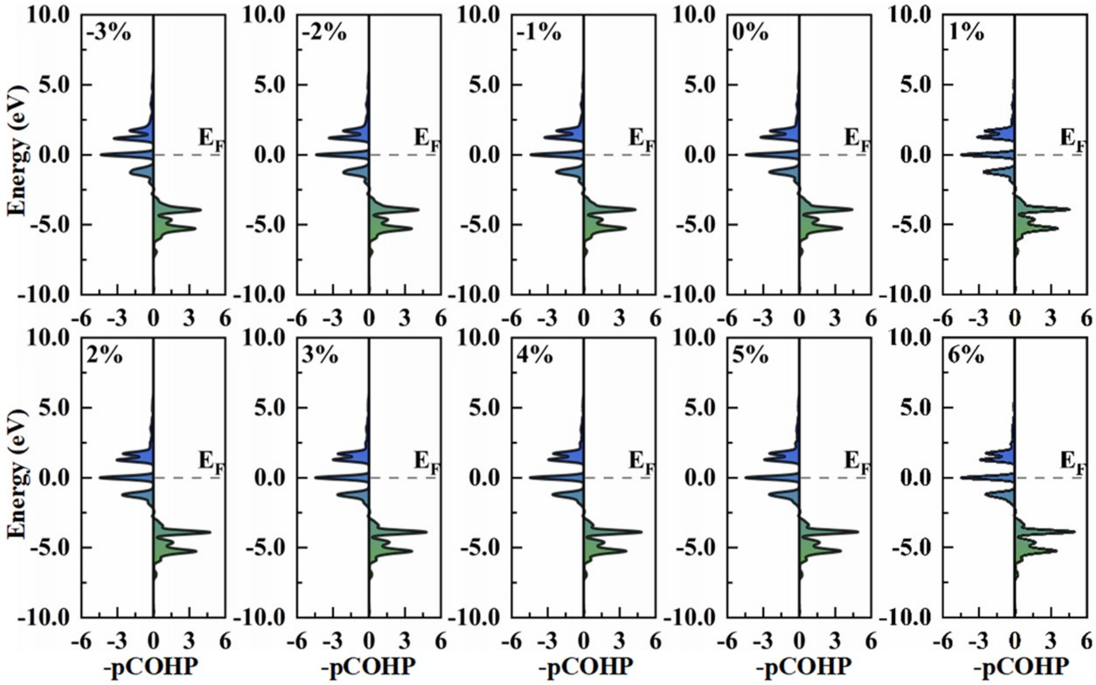

Figure S13. Projected crystal orbital Hamilton population of *O adsorbed Pt@V_{S1}-GaPS$_4$ system under biaxial strain.

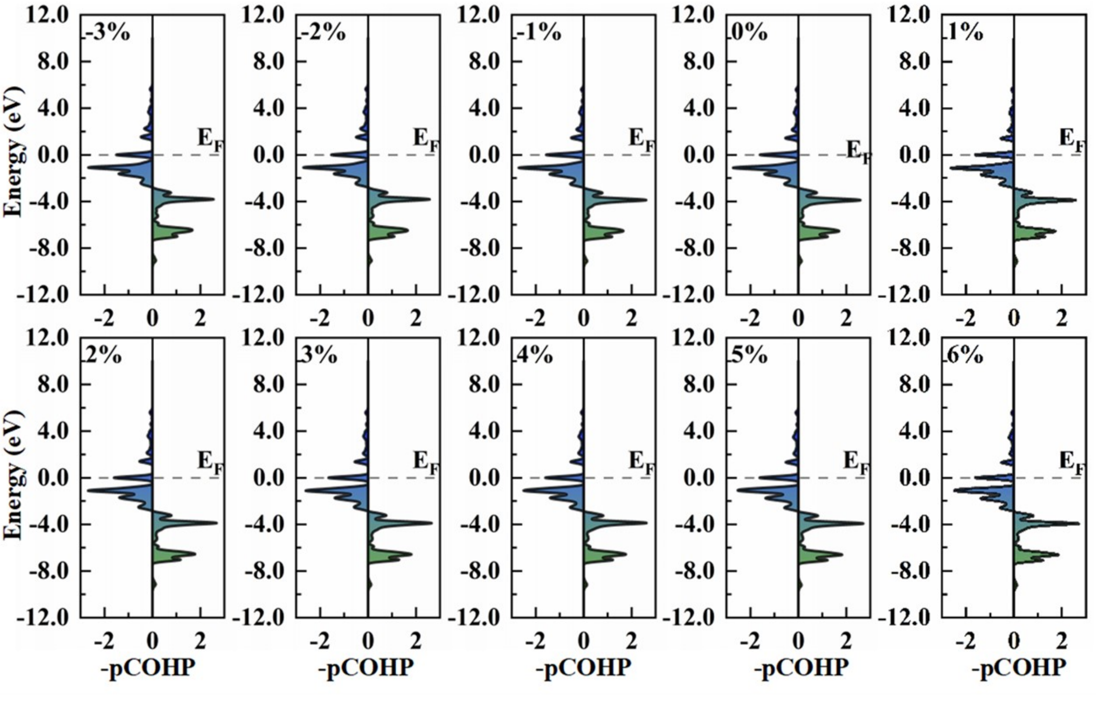

Figure S14. Projected crystal orbital Hamilton population of *OH adsorbed Pt@V_{S1}-GaPS$_4$ system under biaxial strain.

Table S1: The zero-point energy (ZPE) and entropy (S) of adsorption species and the gas molecular of water and hydrogen from the DFT calculation at 298.15 K (T).

Adsorption species	ZPE (eV)	T∆S (eV)
*OH	0.34	0.0
*O	0.07	0.0
*OOH	0.44	0.0
H_2O	0.58	0.67
H_2	0.27	0.41

Table S2: The vacancy formation energies of defective $GaPS_4$.

Vacancy Type	E (eV)
V_{Ga1} - GaPS4	4.13
V_{Ga2} - GaPS4	4.13
V_{P1} - GaPS4	4.24
V_{P2} - GaPS4	2.52
V_{S1} - GaPS4	1.57
V_{S2} - GaPS4	1.62
V_{S3} - GaPS4	1.70
V_{S4} - GaPS4	1.70

Table S3: the bond length between transition metal and P_1 atom (see **Figure 1**), as well as the charge transfer Q_X (x= transition $metal_a$,transition $metal_b$, P_1, OH, O, OOH) in the V_{S1}-$GaPS_4$ system. The negative (-) and positive(+) sign indicate the obtaining and lossing elecrons, respectively. $transition\ metal_b$ and $transition\ metal_a$ represent the transition metal atom after and before adsorbating the (O, OH, OOH), respectively.

transition metal@V_{S1}-$GaPS_4$	Bond length (Å)	Charge transfer (e)						
		transition metal@ V_{S1}-$GaPS_4$	*OH-transition metal@ V_{S1}-$GaPS_4$		*O-transition metal@ V_{S1}-$GaPS_4$		*OOH-transition metal@ V_{S1}-$GaPS_4$	
	$d_{transition\ metal\text{-}P}$	$Q_{transition\ metal}$	$Q_{transition\ metal}$	Q_{*OH}	$Q_{transition\ met}$	Q_{*O}	$Q_{transition\ metal}$	Q_{*OOH}
Au	2.37	+0.09	-0.14	-0.43	+0.21	-0.54	+0.33	-0.59
Co	2.11	+0.10	+0.46	-0.54	+0.32	-0.71	+0.48	-0.57
Cu	2.24	-0.02	+0.13	-0.59	+0.17	-0.94	-0.14	-0.70
Fe	2.13	+0.24	+0.63	-0.49	+0.39	-0.69	+0.45	-0.56
Ir	2.18	-0.27	+0.88	-0.64	+0.88	-0.77	+0.58	-0.62
Mn	2.19	+0.54	+0.57	-0.49	+0.70	-0.66	+0.79	-0.95
Ni	2.08	+0.07	+0.24	-0.58	+0.33	-0.97	+0.32	-0.44
Pt	2.16	+0.24	+0.37	-0.52	+0.56	-0.79	+0.29	-0.46
Re	2.23	+0.93	+0.01	-0.66	+1.10	-0.84	+1.23	-0.70
Rh	2.18	+0.20	+0.42	-0.63	+0.68	-0.80	+0.48	-0.64
Ru	2.16	-0.27	+0.70	-0.63	+1.05	-0.69	+0.71	-0.62

Table S4: In the transition metal@V_{S1}-$GaPS_4$ system, binding energies (E_{bind}) of transition metal/AlP, cohesive energies (E_{coh}) of transition metal atoms in bulk, the computed cluster energies (E_{clus}), the standard dissolution potentials ($U_{diss-bulk}$) of transition metal bulk, the number of transferred electrons (n) during the process of dissolution, and the calculated dissolution potentials (U_{diss}) of transition metal atoms on VN-CN, and the unit of E_{bind}, E_{coh}, E_{clus} are eV, where the unit of $U_{diss-bulk}$ and U_{diss} are V.

system	E_{bind}	E_{coh}	E_{clus}	$U_{diss-bulk}$	n	U_{diss}
Au	-2.96	-3.05	0.10	1.50	3	1.47
Co	-4.29	-5.29	1.01	-0.28	2	-0.78
Cu	-3.14	-4.07	0.93	0.34	2	-0.13
Fe	-6.36	-7.63	1.27	-0.45	2	-1.09
Ir	-6.36	-7.19	0.83	1.16	3	0.88
Mn	-1.97	-4.01	2.05	-1.19	2	-2.21
Ni	-4.73	-5.20	0.48	-0.26	2	-0.50
Pt	-5.79	-5.45	-0.34	1.18	2	1.35
Re	-5.37	-7.83	2.47	0.30	3	-0.52
Rh	-5.98	-6.40	0.42	0.60	2	0.39
Ru	-6.11	-7.28	1.16	0.46	2	-0.12

Table S5: In the V_{S1}-$GaPS_4$ system, the free energy changes between two intermediate processes, slab to OH (ΔG_1), OH to O (ΔG_2), OOH to O (ΔG_3) and O_2 to OOH (ΔG_4) of transition metal/AlP system, as well as the corresponding OER overpotential (η_{OER}) and ORR overpotential (η_{ORR}).

transition metal-based system	ΔG_1 (eV)	ΔG_2 (eV)	ΔG_3 (eV)	ΔG_4 (eV)	η_{OER} (V)	η_{ORR} (V)
Au	-1.39	1.10	-0.93	6.14	1.22	1.39
Co	-1.74	-0.14	0.84	5.95	1.03	1.74
Cu	-2.04	0.11	0.85	6.00	1.08	2.04
Fe	-1.36	-0.40	0.87	5.80	0.88	1.36
Ir	-1.96	-0.03	0.77	6.15	1.23	1.96
Mn	-2.33	-1.02	1.04	7.22	2.30	2.33
Ni	-1.25	-0.60	1.70	5.07	1.70	1.25
Pt	0.59	0.41	0.24	4.86	0.41	0.59
Re	-2.35	-0.88	1.60	6.54	1.62	2.35
Rh	-1.52	0.28	0.80	5.36	0.80	1.52
Ru	-1.38	-0.64	1.22	5.72	1.22	1.38

Table S6. The free energy (*G*) of gas $O_{2(g)}$, $H_{2(g)}$ and liquid water H_2O (l) at 1/0.035 bar and 298.15 K, E presents the free energy calculated from DFT, and ΔG is the Frequency correction energy.

Molecular	Pressure/bar	Temperature/ K	E(DFT)/eV	ΔG/eV	G/eV
$O_{2(g)}$	1	298.15	--	--	-9.91
$H_{2(g)}$	1	298.15	-6.76	-0.045	-6.8
$H_2O_{(l)}$	0.035	298.15	-14.22	-0.001	-14.22

Table S7: the d-band center (in eV) of transition metal in the V_{S1}-$GaPS_4$ system, where Spin up and Spin down are the d-band center of spin-up and spin-down electrons, and Average stands for the mean of the two values. μ_B is the magnetic moment.

transition metal	Spin up	Spin down	Average	μ_B
Au	-3.74	-3.61	-3.67	1.00
Co	-1.25	-0.31	-0.79	1.00
Cu	-2.70	-2.59	-2.64	1.00
Fe	-1.70	0.17	-0.78	2.00
Ir	-1.92	-1.57	-1.75	1.00
Mn	-1.08	0.29	-0.41	1.00
Ni	-0.78	-0.77	-0.78	0.00
Pt	-1.52	-1.52	-1.52	0.00
Re	-0.93	-0.46	-0.70	1.00
Rh	-1.74	-1.37	-1.56	1.00
W	-0.50	-0.50	-0.50	0.00

Table S8: In the transition metal@V_{S1}-$GaPS_4$ system, the inter-atomic charge transfer in transition metal, O, H among each adsorption process, where $Q_{transition\ metal}$, Q_O and Q_H are the value of charge transfer in transition metal, O and H atoms after absorbing the OH, and $Q_{transition\ metal}'$, Q_O', Q_H' are the quantities of charge transfer in transition metal and O atom in *O process, and the $Q_{transition\ metal}''$, Q_{O_1}'', Q_{O_2}'', Q_H'' represent the number of charge transfer in transition metal, O, and H atoms in *OOH process.

	$Q_{transition\ metal}$ * OH			$Q_{transition\ metal}$ * O		$Q_{transition\ metal}$ * OOH			
transition metal-based system	$Q_{transition\ metal}$	Q_O	Q_H	$Q_{transition\ metal}'$	Q_O'	$Q_{transition\ metal}''$	Q_{O_1}''	Q_{O_2}''	Q_H''
Au	-0.14	-0.61	+0.18	+0.21	-0.54	+0.33	-0.52	-0.50	+0.42
Co	+0.46	-0.75	+0.21	+0.32	-0.71	+0.48	-0.43	-0.51	+0.37
Cu	+0.13	-0.84	+0.25	+0.17	-0.94	-0.14	-0.54	-0.48	+0.33
Fe	+0.63	-0.68	+0.19	+0.39	-0.69	+0.45	-0.46	-0.38	+0.28
Ir	+0.88	-0.90	+0.26	+0.88	-0.77	+0.58	-0.56	-0.53	+0.47
Mn	+0.57	-0.59	+0.10	+0.70	-0.66	+0.79	-0.58	-0.64	+0.26
Ni	+0.24	-0.93	+0.34	+0.33	-0.97	+0.32	-0.45	-0.44	+0.45
Pt	+0.37	-0.76	+0.24	+0.56	-0.79	+0.29	-0.47	-0.39	+0.40
Re	+0.01	-0.57	-0.09	+1.10	-0.84	+1.23	-0.57	-0.13	0.00
Rh	+0.42	-0.79	+0.17	+0.68	-0.80	+0.48	-0.56	0.00	+0.08
Ru	+0.70	-0.79	+0.16	+1.05	-0.69	+0.71	-0.53	-0.54	+0.45

Table S9: In the transition metal@V_{S1}-$GaPS_4$ system, the adsorption energy of OH, O, OOH (ΔG_{*OH}, ΔG_{*O}, ΔG_{*OOH}).

transition metal-based system	ΔG_{*OH} (eV)	ΔG_{*O} (eV)	ΔG_{*OOH} (eV)
Au	-0.16	2.17	2.47
Co	-0.51	0.58	2.66
Cu	-0.81	0.53	2.61
Fe	-0.13	0.71	2.81
Ir	-0.73	0.47	2.46
Mn	-1.10	-0.88	1.39
Ni	-0.02	0.61	3.54
Pt	0.64	2.28	3.75
Re	-1.12	-0.76	2.07
Rh	-0.29	1.22	3.25
Ru	-0.15	0.44	2.89

Table S10. The descriptors related to structure and atomic properties, including the bond length of transition metal and circumambient atoms ($d_{\text{transition metal-S2}}$ (d_1), $d_{\text{transition metal-S1}}$ (d_2), $d_{\text{transition metal-Ga2}}$ (d_3), and $d_{\text{transition metal-P}}$ (d_4), Å), the d-band center (ε_d, eV), the electronegativity (N_m), the electron affinity (χ_m, eV), the first ionization energy (I_m, eV), the radius of transition metal atom (r_d, pm), the bond angle of transition metal and the Ga_1 and Ga_3 atoms (θ, the θ is radians), and the number of transition metal-d electrons (N_e).

transition metal	d_1 (Å)	d_2 (Å)	d_3 (Å)	d_4 (Å)	ε_d (eV)	N_m	χ_m (eV)	I_m (eV)	r_d (pm)	θ	N_e
Au	3.58	3.7	2.5	2.37	-3.67	2.4	2.31	9.23	1.44	1.98	10
Co	2.22	4.79	2.34	2.11	-0.79	1.9	0.66	7.88	1.26	2.08	7
Cu	2.27	4.93	2.42	2.24	-2.649	1.9	1.23	6.84	1.28	2.01	10
Fe	2.25	4.89	2.41	2.13	-0.789	1.8	0.16	7.9	1.27	2.17	6
Ir	2.33	4.56	2.42	2.18	-1.795	2.2	1.57	9.12	1.36	2.04	7
Mn	2.14	4.72	2.48	2.19	-0.41	1.5	-0.50	7.43	1.32	2.08	5
Ni	2.2	5.16	2.35	2.08	-0.78	1.8	1.16	7.64	1.24	2.23	8
Pt	3.65	3.74	2.42	2.16	-1.52	2.2	2.13	8.96	1.39	2.09	9
Re	2.21	4.45	2.53	2.23	-0.70	1.9	0.15	7.88	1.37	2.26	5
Rh	2.35	4.59	2.42	2.18	-1.56	2.2	1.14	7.46	1.34	2.03	8
Ru	2.20	4.50	2.44	2.16	-0.57	2.2	1.05	7.36	1.32	2.07	7

Table S11: The charge transfer in strained Pt@V_{S1}-$GaPS_4$ system. The positive (negative) indicates losing (obtaining) electrons. where Q_{Pt}, Q_O and Q_H are the value of charge transfer in transition metal, O and H atoms after absorbing the OH, and Q_{Pt}', Q_O', Q_H' are the quantities of charge transfer in transition metal and O atom in *O process, and the Q_{Pt}'', Q_{O_1}'', Q_{O_2}'', Q_H'' represent the number of charge transfer in transition metal, O, and H atoms in *OOH process.

adsorptions	Q_{Pt*OH}			Q_{Pt*O}		Q_{Pt*OOH}			
stress	Q_{Pt}	Q_O	Q_H	Q_{Pt}'	Q_O'	Q_{Pt}''	Q_{O_1}''	Q_{O_2}''	Q_H''
-3%	+0.31	-0.98	+0.43	-0.02	-0.74	+0.22	-0.46	-0.62	+0.62
-2%	+0.38	-0.86	+0.29	+0.38	-0.77	+0.01	-0.54	-0.24	+0.37
-1%	+0.46	-0.84	+0.31	+0.48	-0.78	+0.51	-0.45	-0.41	+0.44
0%	+0.37	-0.76	+0.24	+0.56	-0.79	+0.29	-0.47	-0.39	+0.40
1%	+0.10	-0.74	+0.26	+0.63	-0.79	+0.56	-0.48	-0.42	+0.44
2%	0.00	-0.82	+0.30	+0.47	-0.78	-0.33	-0.52	-0.34	+0.37
3%	-0.05	-0.85	+0.34	+0.55	-0.78	+0.48	-0.48	-0.51	+0.51
4%	-0.42	-0.72	+0.32	+0.64	-0.79	+0.37	-0.48	-0.38	+0.41
5%	-0.65	-0.55	+0.09	+0.42	-0.75	+0.54	-0.49	-0.42	+0.44
6%	+0.15	-0.82	+0.30	+0.57	-0.72	-0.06	-0.41	-0.28	+0.33

Table S12: When the biaxial strain is applied to the Pt@V_{S1}-$GaPS_4$ system, the correlation Angle α of transition metal atoms, the sum of bond angles θ, and the deviation degree δ for no strain action.

angle	α (°)				θ (°)	δ (°)
stress	α_1	α_2	α_3	α_4	$\alpha_1 + \alpha_2 + \alpha_3 + \alpha_4$	α_{OH}
-3%	119.89	114.69	105.69	76.97	417.24	0.43
-2%	119.27	115.16	105.97	76.78	417.18	0.37
-1%	119.18	115.22	105.95	76.91	417.26	0.45
0%	118.75	115.08	106.30	76.68	416.81	0.00
1%	118.62	114.76	106.55	76.57	416.50	-0.31
2%	118.6	115.13	106.75	76.30	416.78	-0.03
3%	117.96	114.37	107.45	75.94	415.72	-1.09
4%	118.31	115.86	106.77	76.33	417.27	0.46
5%	118.33	116.80	106.51	76.54	418.18	1.37
6%	118.50	116.28	106.72	76.45	417.95	1.14

Table S13: Applying biaxial strain in Pt@V_{S1}-$GaPS_4$ system, the free energy changes between two intermediate processes, slab to OH ΔG_1 (), OH to O (ΔG_2), OOH to O (ΔG_3) and O_2 to OOH (ΔG_4) of transition metal/$GaPS_4$ system, as well as the corresponding OER overpotential (η_{OER}) and ORR overpotential (η_{ORR}).

stress	ΔG_1 (eV)	ΔG_2 (eV)	ΔG_3 (eV)	ΔG_4 (eV)	η_{OER} (V)	η_{ORR} (V)

-3%	-0.74	0.52	0.17	0.06	0.52	0.74
-2%	-0.71	0.47	0.18	0.06	0.47	0.71
-1%	-0.66	0.44	0.20	0.02	0.44	0.66
0%	-0.59	0.41	0.23	-0.06	0.41	0.59
1%	-0.51	0.39	0.29	-0.18	0.39	0.51
2%	-0.43	0.40	0.26	-0.23	0.40	0.43
3%	-0.28	0.33	0.31	-0.37	0.33	0.37
4%	-0.24	0.41	0.31	-0.48	0.41	0.48
5%	-0.14	0.42	0.31	-0.59	0.42	0.59
6%	-0.02	0.42	0.28	-0.69	0.42	0.69

Table S14: The Charge transfer of doped Pt atom (Q_{Pt}) under different strains and the positive (negative) indicates losing (obtaining) electrons. the d-band center (in eV) of Pt in the V_{S1}-$GaPS_4$ system, where Spin up and Spin down are the d-band center of spin-up and spin-down electrons, and Average stands for the mean of the two values. μ_B is the magnetic moment.

stress	Q_{Pt}	Spin up	Spin down	Average	μ_B
-3%	-0.36	-1.61	-1.61	-1.61	0.00
-2%	-0.37	-1.58	-1.58	-1.58	0.00
-1%	-0.05	-1.55	-1.55	-1.55	0.00
0%	+0.25	-1.52	-1.52	-1.52	0.00
1%	-0.23	-1.51	-1.51	-1.51	0.00
2%	-0.12	-1.49	-1.49	-1.49	0.00
3%	+0.07	-1.49	-1.49	-1.49	0.00
4%	-0.05	-1.48	-1.48	-1.48	0.00
5%	-0.07	-1.50	-1.50	-1.50	0.00
6%	-0.04	-1.49	-1.49	-1.49	0.00

References:

1. Nørskov, J. K.; Rossmeisl, J.; Logadottir, A.; Lindqvist, L., Origin of the Overpotential for Oxygen Reduction at a Fuel-Cell Cathode. *J. Phys. Chem. B* **2004,** *108*, 17886-17892.
2. Niu, H.; Wang, X.; Shao, C.; Liu, Y.; Zhang, Z.; Guo, Y., Revealing the oxygen reduction reaction activity

origin of single atoms supported on g-C3N4 monolayers: a first-principles study. *J. Mater. Chem. A* **2020,** *8* (14), 6555-6563.

3. Guo, H.; Zhang, Z.; Huang, B.; Wang, X.; Niu, H.; Guo, Y.; Li, B.; Zheng, R.; Wu, H., Theoretical study on the photocatalytic properties of 2D InX(X = S, Se)/transition metal disulfide (MoS2 and WS2) van der Waals heterostructures. *Nanoscale* **2020,** *12* (38), 20025-20032.
4. Holby, E. F.; Wang, G.; Zelenay, P., Acid Stability and Demetalation of PGM-Free ORR Electrocatalyst Structures from Density Functional Theory: A Model for "Single-Atom Catalyst" Dissolution. *ACS Catal.* **2020,** *10* (24), 14527-14539.
5. Guo, X.; Lin, S.; Gu, J.; Zhang, S.; Chen, Z.; Huang, S., Simultaneously Achieving High Activity and Selectivity toward Two-Electron O2 Electroreduction: The Power of Single-Atom Catalysts. *ACS Catal.* **2019,** *9* (12), 11042-11054.
6. Niu, H.; Zhang, Z.; Wang, X.; Wan, X.; Shao, C.; Guo, Y., Theoretical Insights into the Mechanism of Selective Nitrate-to-Ammonia Electroreduction on Single-Atom Catalysts. *Adv. Funct. Mater.* **2020,** *31* (11), 2008533.
7. Friedman, J. H., Stochastic Gradient Boosting. *Comput. Stat. Data. Anal.* **2002,** 38(4), 367-378.
8. Friedman, J. H., Greedy Function Approximation: a Gradient Boosting Machine. *Ann. Stat.* 2001, 29(5), 1189-1232.